View metadata, citation and similar papers at core.ac.uk
brought to you by CORE
provided by NASA Technical Reports Server

N89-27912

Why is CDMA the Solution for Mobile Satellite Communication ?

by
Klein S. Gilhousen, Irwin M. Jacobs,
Roberto Padovani, and Lindsay A. Weaver[1]

Introduction

This paper will demonstrate that spread spectrum CDMA systems provide an economically superior solution to satellite mobile communications by increasing the system maximum capacity with respect to single channel per carrier FDMA systems. Following the comparative analysis of CDMA and FDMA systems, the paper describes the design of a modem that was developed to test the feasibility of the approach and the performance of a spread spectrum system in a mobile environment. Results of extensive computer simulations as well as laboratory and field tests results are presented.

The BER of the rate 1/3, constraint length 9, convolutionally encoded BPSK modem proved to be within 0.3 dB from theory in a AWGN channel, thus achieving a BER of 10^{-3}, adequate for voice, at Eb/No=2.5 dB. The powerful convolutional code combined with interleaving and a robust modulation also provide excellent performance in Rician fading and lognormal shadowing.

The paper is organized as follows. In Section I, a review of previous comparisons of the maximum throughput achievable by CDMA and FDMA systems is given. In Section II, the comparisons between CDMA and FDMA are rederived for mobile satellite systems. In Section III, a description of the spread-spectrum modem and the performance results are given.

I. Spectral Efficiency of CDMA and FDMA

In [1], Viterbi compared the spectral efficiency of CDMA and FDMA as a function of total carrier-to-noise power ratio. The comparison was carried out for uncoded BPSK (QPSK) as well as convolutionally coded systems with various code rates. We review here the main results of [1]. The spectral efficiency for BPSK CDMA is given by

$$\eta = \frac{\frac{C}{N_o W_s}}{\frac{E_b}{N_o}} = \frac{\frac{C}{N_o W_s}}{\frac{E_b}{N_o+I_o}\left(1+\frac{C}{N_o W_s}\left(\frac{M-1}{M}\right)\right)}$$

[1] The authors are with Qualcomm, Inc. San Diego, CA 92121. This work was partially supported by Hughes Aircraft Company. Portions of this paper were presented at the Mobile Satellite Conference in Pasadena, May 1988.

$$\approx \frac{\frac{C}{N_o W_s}}{\frac{E_b}{N_o+I_o}(1+\frac{C}{N_o W_s})} \quad \text{bits/sec/Hz} \qquad (1)$$

where:

C = Total carrier power.

W_s = Total occupied bandwidth.

$\frac{E_b}{N_o+I_o}$ = Bit Energy/Single sided Total Noise spectral density, required for given BER.

N_o = Single sided Thermal Noise spectral density.

I_o = Single sided Other Users Noise spectral density.

M = Number of users in the system.

For a single channel per carrier FDMA system, there is only one user per bandwidth segment, therefore $E_b/(N_o+I_o) = E_b/N_o$ and (1) becomes

$$\eta = \frac{\frac{C}{N_o W_s}}{\frac{E_b}{N_o}} \qquad \text{if} \frac{MR_b}{W_s} < r \log_2(m) \quad G_{FDMA} \qquad (2)$$

and due to the bandwidth limit

$$\eta = r \log_2(m)\, G_{FDMA} = \max h_{FDMA} \qquad \text{if } \frac{MR_b}{W_s} \geq r \log_2(m)\, G_{FDMA} \qquad (3)$$

where

r = Code rate.

m = Signal constellation dimension (m=2 for BPSK, m=4 for QPSK, etc.).

R_b = Each User's information rate.

G_{FDMA} = FDMA Guardband factor.

Asymptotically, as $C/N_o W_s \rightarrow \infty$, the efficiencies of the CDMA and FDMA systems are

$$\text{MAX } \eta_{CDMA} = \frac{1}{\frac{E_b}{N_o+I_o}},$$

$$\text{MAX } \eta_{FDMA} = r \log_2(m)\, G_{FDMA}. \qquad (4)$$

The spectral efficiencies as given by Eqs. (2) and (3) are shown in Fig. 1 for two representative systems transmitting 4800 bps and achieving a BER of 10^{-3} on a AWGN channel. The first is a spread spectrum CDMA system with a rate 1/3 K=9 convolutional code and $E_b/(N_o+I_o)$= 2.5 dB. The FDMA system is the rate 2/3 trellis coded 8-DPSK, proposed in [3], with Eb/No = 8.4 dB.

The FDMA guardband factor allows margin for adjacent channel interference. For the purpose of comparison, we will assume the 5 KHz channelization of the L-band

spectrum assigned to mobile services, as proposed by the American Mobile Satellite Consortium (AMSC) in [4]. Thus, in the previous example $G_{FDMA} \approx 0.5$, i.e an octal symbol rate of 2400 sps in the 5 KHz channel [1].

It is seen from Fig. 1 that the FDMA system capacity is about twice the capacity achieved by the CDMA system, in agreement with the conclusions of [1], i.e. " When C/No is at premium don't contribute further to the noise by having the users jam one another ".

II. CDMA vs. FDMA: The Mobile Satellite Channel

The conclusion of the comparison developed in Section I will be *reversed* when the two systems are compared in a mobile satellite environment [2]. The four major factors that alter the result of the comparison are:

(1) voice activity,
(2) spatial discrimination provided by satellite steerable array antennas,
(3) crosspolarization attenuation,
(4) and multiple satellites.

Voice services will likely occupy up to 95% of the mobile communication channels; the voice activity factor will greatly reduce the self-noise of the spread spectrum system. The voice services will use voice activated carrier transmission, which means that when a user is listening or pausing during a conversation the carrier is turned off and thus does not contribute to the system self-noise. Conventional telephone practice [5] for satellite circuits indicates that a given user will only be talking approximately 35% of the time. In FDMA , on the other hand, the voice activity factor does not increase the capacity when the system is bandwidth limited but only reduces the necessary satellite transmitted power when operating in a power limited mode. This has the effect of shifting the FDMA efficiency curve of Fig. 1 to the left by the voice activity factor, i.e. by 4.56 dB for a 35% activity factor.

The capacity of the CDMA system is further improved by multiple beams satellite antennas. For example, the coverage shown in Fig. 2 may be used by first generation satellites. The performance of the CDMA system is governed by the ratio E_b/I_o, assuming that I_o is greater than N_o, a fair assumption for the system under consideration. On the mobile-to-satellite link, the value of I_o is equal to the total signal power, from all active terminals, received by the satellite antenna, weighted by the antenna beam pattern. Equivalent to the concept of "noise bandwidth" in linear filters we can define an "equivalent noise beamwidth" B of the antenna, where

$$B = \int_{-\pi/2}^{\pi/2} G(q)\, dq,$$

and G(q) is the antenna gain. For example, with a 7 x 2.5 meter antenna B = 1.4° and assuming a uniform distribution of users within the continental U.S., the worst case beam will receive only about 20 % of the total interference. This means that the value of I_o is reduced by 7 dB, i.e. a direct equivalent increase in system capacity.

[1] It should be pointed out that a smaller guardband factor could be achieved with sharper filtering. In this example, we chose to compare the system proposed in [2] which uses a 100% roll-off factor. If a smaller roll-off is used, then the FDMA spectral efficiency increases accordingly.

The FDMA system will also gain from the use of such an antenna. The antenna coverage can be designed to provide frequency reuse every 3°, namely the frequencies can be reused every fourth beam. Assuming a uniform user distribution over the continental U.S., Fig. 2 indicates that the full spectrum can be used twice; thus the FDMA capacity is doubled. A much larger antenna [6], considered for satellites of later generations, could provide a fourfold frequency reuse.

The CDMA system can also reuse the entire frequency band by utilizing the two opposite senses of circular polarization. The frequency reuse is possible because the I_o affecting a given channel is the sum of the I_o generated by the users with the same polarization plus the I_o generated by the users of opposite polarization *attenuated by the crosspolarization factor,* plus the reflected paths of the users of opposite polarization.

On the other hand, polarization isolation cannot be exploited by a FDMA system. In the FDMA system, a signal path that is reflected, will be jamming at full strength the user on the opposite sense of polarization and at the same frequency.

Considering the above modifications, we can now recalculate the spectral efficiencies as a function of average carrier to noise power for the two system previously considered. The value of the total noise, thermal plus other users, affecting a CDMA user, taking into account voice activity, antenna discrimination, and crosspolarization attenuation, can be calculated as follows

$$N_o + I_o = N_o + a\rho V(M-1)E_c \tag{5}$$

where

a = Antenna discrimination factor = 20%

ρ = Polarization reuse factor = $\dfrac{1+\text{Crosspolarization Attenuation}}{2}$

(a crosspolarization attenuation = 10 dB is assumed)

V = Voice activity factor = 35%

E_c = Received energy in one spread spectrum pseudo-noise chip.

The average carrier-to-noise power is given by

$$\frac{C}{N_o W_s} = VM\frac{R_b}{W_s}\frac{E_b}{N_o}; \tag{6}$$

thus the spectral efficiency is

$$\eta_{CDMA} = \frac{MR_b}{W_s} = \frac{\frac{C}{N_o W_s}}{V\frac{E_b}{N_o}} = \frac{\frac{C}{N_o W_s}}{V\frac{E_b}{N_o+I_o}\left(1 + a\rho\frac{C}{N_o W_s}\left(\frac{M-1}{M}\right)\right)}$$

$$\approx \frac{\frac{C}{N_o W_s}}{V\frac{E_b}{N_o+I_o}\left(1 + a\rho\frac{C}{N_o W_s}\right)} \tag{7}$$

Asymptotically, for $C/N_oW_s \to \infty$, Eq.(7) becomes

$$\text{Max } \eta_{CDMA} = \frac{1}{Va\rho\frac{E_b}{N_o+I_o}} \tag{8}$$

The spectral efficiency of the FDMA system in the power limited region becomes

$$\eta_{FDMA} = 2\frac{\frac{C}{N_o W_s}}{V\frac{E_b}{N_o}} \tag{9}$$

where the factor of two accounts for the frequency reuse. Asymptotically, in the bandwidth limited region Eq.(9) becomes

$$\text{Max } \eta_{FDMA} = 2\, r \log_2(m)\, G_{FDMA} \tag{10}$$

The spectral efficiencies calculated in Eq.(7) and (9) are shown in Fig.3. Again, the CDMA system assumes a $E_b/(N_o+I_o)$ = 2.5 dB and the FDMA system a E_b/N_o = 8.4 dB. The ratio of the asymptotic values is

$$\frac{\text{Max } \eta_{CDMA}}{\text{Max } \eta_{FDMA}} = \frac{\frac{1}{Va\rho\frac{E_b}{N_o+I_o}}}{2\, r \log_2(m)\, G_{FDMA}} = 7.3 \tag{11}$$

The result of Eq.(11) clearly indicates the superiority of the CDMA approach. Table I shows a link budget for both systems. The results of the link budgets reflect the behavior of Fig. 3 and show a threefold greater capacity of the CDMA system with respect to the FDMA system, for a realistic value of $C/N_o W_s$. The details and assumptions that led to the link budget of Table 1 are given in Appendix I.

The link budget of Table I and the results of Fig.3 indicate that the CDMA system could achieve even higher capacity whereas the capacity of the FDMA system becomes limited by the bandwidth requirement. Multiple satellites provide a way of improving the CDMA capacity versus FDMA even more. Use of CDMA will allow coherent combining of signals transmitted between a terminal and all satellites in view. The coherent combining will result in an effective capacity gain corresponding to the increased number of satellites. On the other hand, a FDMA system already in a bandwidth limited mode, will not benefit from additional satellites unless every mobile terminal is equipped with a costly directive antenna. An alternative to the directive antenna approach, could be a higher modulation level, e.g. 16-PSK, thus taking advantage of the extra power provided by the additional satellites; even in this case though FDMA would fall short in comparison with CDMA.

III. Performance of a Direct Sequence Spread Spectrum Modem in the Mobile Environment

Recently, several studies [7]-[10] have been conducted to characterize the propagation effects for mobile satellite communications. A generally agreed upon

conclusion is that the channel can be approximated by a Rician distribution, with a ratio of specular to diffuse component K=10 dB, and lognormal distributed shadowing process affecting the direct path. In [7] a best fit to measured data affected by shadowing conditions, was found with a lognormal distribution with mean value =-7.5 dB and a standard deviation of 3 dB. This model is shown in Fig. 4. With the above assumption, the received signal can be expressed as follows

$$r(t) = \mathrm{Re}\ \{\ x(t)\ e^{j(2\pi F_c t+\theta)}\ \}$$

where the complex envelope x(t) is given by

$$x(t) = z(t)\ d(t) + w(t). \tag{12}$$

Here the quantity d(t) can be expressed as,

$$d(t) = \sqrt{E_S} \sum_{i=-\infty}^{\infty} a_i\ p(t-iT) \tag{13}$$

where the a_i's represent the binary $\pm$ 1 data sequence, p(t) is the channel pulse, and E_S represents the signal energy per coded symbol, i.e. $E_S = rE_b$ with r the code rate. In Eq. (12), w(t) represents a stationary zero-mean complex Gaussian process with in-phase and quadrature components with single-sided spectral density N_o. The process z(t) combines the effects of fading and shadowing. The process z(t) can be expressed in terms of its real and imaginary part as follows

$$z(t) = [s(t) + i(t)] + j\ q(t), \tag{14}$$

where i(t) and q(t), representing the Rayleigh fading, are wide sense stationary zero-mean Gaussian random processes with spectral density R(f) and variance 1/2K, and s(t) represents the shadowing process. The random process s(t) can be expressed more conveniently as

$$s(t) = 10^{(\gamma(t) + m_S)/20}, \tag{15}$$

where $\gamma(t)$ is a zero-mean stationary Gaussian process with spectral density $R_\gamma(f)$ and standard deviation σ = 3 dB and m_S = - 7.5 dB. Throughout the rest of the paper we will assume that R(f) and $R_\gamma(f)$ are 6-th order Butterworth spectra with cutoff frequencies F_c = 10 cycles/meter and F_c = 5 cycles/meter respectively, i.e. corresponding to bandwidths of 150 Hz and 75 Hz at a vehicle speed of 15 meter/sec. With the above assumptions, the in-phase and quadrature components of the output of the matched filter are

$$r_k^{(I)} = \sqrt{\frac{2E_S}{N_o}}\ a_k\ [\ (s_k+i_k)\cos(\theta) + q_k\sin(\theta)\ ]\ + w_k^{(I)}$$

$$r_k^{(Q)} = \sqrt{\frac{2E_S}{N_o}}\ a_k\ [\ q_k\cos(\theta) - (s_k+i_k)\sin(\theta)\ ]\ + w_k^{(Q)} \tag{16}$$

Notice that in Eq. (16) the noise variables have been normalized to unit variance and that in the absence of shadowing, i.e. $s_k = 1$, Eq. (16) represents a Rician channel.

The feasibility of the CDMA approach to mobile communications was tested through the development of a direct sequence spread spectrum modem capable of supporting four data rates 2400, 4800, 9600, and 16000 bps.

The coded BPSK modem was designed to occupy a 9 MHz bandwidth with a chip rate of 8 Mcps, corresponding to spread spectrum processing gains of 35.3 dB, 32.3 dB, 29.2 dB, and 27 dB for the respective four data rates. A rate 1/3 constraint length K=9 convolutional code with Viterbi decoding was used which provides a coding gain of 4.5 dB at a BER=10^{-3}.

Interleaving following the convolutional encoder and deinterleaving prior to the Viterbi decoder is a necessary operation in a fading environment. The interleaver, in this case a block interleaver was chosen, has the effect of spreading adjacent coded symbols affected by fading, thus allowing the Viterbi decoder to correct most of the errors generated by the fades. Since voice transmission is the primary application of the system, long interleaver depths cannot be used, since additional delays are introduced. A simulation was performed to evaluate the effects of different interleaving depths; the fading model used was the one shown in Fig.4. The results are summarized in Fig.5 which shows the cumulative fade depth probability for two interleaver depths, namely 0.26 meter and 0.50 meters, corresponding to 25 msec and 50 msec at a vehicle speed of about 35 Kmh, and for the case where no interleaver is used. Since a 50 msec interleaver generates an additional 100 msec delay which was considered excessive for voice communication, the 0.26 meter interleaver was selected. At a vehicle speed of 15 Kmh, a full 25 msec vocoder frame was interleaved.

In order to ease the acquisition process of the mobile units a pilot signal was added to the data generated by the vocoder. In contrast with the user data, which is spread by means of a long PN sequence, the pilot signal consists of an unmodulated short PN sequence of length 4095. The low power pilot, which is always present for mobile units to acquire on, provides an excellent mean of fast acquisition without degrading the capacity of the system. A pilot $E_C/(N_O+I_O)$ = - 20 dB degrades system capacity by only 0.3 dB, as shown in Table I, while assuring rapid acquisition and practically perfect tracking performance.

In the mobile-to-hub link, the pilot signal was replaced by short preambles preceding every vocoder frame. The preambles are used to acquire frequency, phase, timing as well as signal levels of the mobile units. This link was also provided with a DPSK fall-back modulation mode to be used when fading conditions do not allow coherent demodulation.

Laboratory measurements were conducted to test the BER of the modem. A channel fading simulator, as shown in Fig.4, was used to simulate the fading and shadowing processes. Amongst other parameters the channel simulator allows the operator to simulate a given vehicle speed by selecting the appropriate bandwidths of the fading and shadowing processes.

The BER performance of the modem are shown in Fig.6 and 7 for both directions of the link. From Figs. 6 and 7 it is clear that the hub-to-mobile link is more robust. The reason is twofold. First the presence of the pilot signal allows the mobile to track the faded carrier with little degradation. Secondly, in the hub-to-mobile link, when the signal is shadowed so is the interference from the other users, whereas in the mobile-

to-hub link when the wanted signal is shadowed the interference from the other users may not be. A ratio of I_O/N_O=10 dB was always assumed in the tests.

A degradation of 6.3 dB is observed in the mobile unit in faded and shadowed conditions, K=10, m_S=-7.5 dB, σ=3 dB, and a vehicle speed of 48 Kmh. A degradation of 8.6 dB was observed in the mobile-to-hub link for the same channel conditions in the DPSK mode.

The modem was implemented with a single TMS32020 digital signal processor in six 5.2 x 1.6 cm wirewrap boards clearly indicating the feasibility and cost effectiveness of the approach.

Extensive field tests were also performed and the results are reported in [11]. The major conclusions of the field tests were that in all conditions the mobile-to-hub link never needed to fall back to the DPSK mode, when the BPSK mode was provided with a link margin of 2 dB, and that such a link margin proved to be sufficient to provide good quality voice in both directions.

Conclusions

This paper proved that CDMA systems provide greater capacity than FDMA for mobile satellite communications. Often CDMA is dismissed as a viable approach for mobile satellite communications and the results of [1] are used to argue in favour of FDMA systems. We have shown that although the conclusions of [1] still hold, several factors that apply to mobile communication services can be exploited by a CDMA system thus shifting the results of the comparison with FDMA in favour of a CDMA approach. This paper shows that the capacity of a CDMA system is asymptotically about 7 times greater than a FDMA system currently proposed and about 3 times greater when compared using current estimates for available satellite EIRP, antenna gains, etc.

The feasibility of a direct sequence spread spectrum approach to mobile communications has been tested through the development of a modem capable of supporting digitized voice at four different rates. Performance results are reported here and results of a comparative test with an ACSSB modem are reported in [11] as well as the results of a test of the spread spectrum modem conducted at C-Band using an existing satellite.

References

[1] A.J. Viterbi, " When Not to Spread Spectrum - A Sequel, "IEEE *Communication Magazine*, Vol. 23, pp. 12-17, Apr 1985.

[2] I.M. Jacobs et al., "Comparison of CDMA and FDMA for the MobileStar(sm) System," *Proceedings of the Mobile Satellite Conference*, pp. 283-290, May 3-5 1988, Pasadena.

[3] D. Divsalar and M.K. Simon, "Trellis Coded MPSK Modulation Techniques for MSAT-X," *Proceedings of the Mobile Satellite Conference*, pp. 283-290, May 3-5 1988, Pasadena.

[4] C.E. Agnew et al., "The AMSC Mobile Satellite System," *Proceedings of the Mobile Satellite Conference*, pp. 3-10, May 3-5 1988, Pasadena.

[5] J.M. Fraser, "Engineering Aspects of TASI," *Bell System Tech. Journal*, Vol. 38, pp. 353-365, Mar 1959.

[6] W. Rafferty, K. Dessouky, and M. Sue, "NASA's Mobile Satellite Development Program," *Proceedings of the Mobile Satellite Conference*, pp. 11-22, May 3-5 1988, Pasadena.

[7] J.S. Butterworth, "Propagation Measurements for Land Mobile Satellite Systems at 1542 MHz," *Communications Research Centre*, Technical Note No. 723, Department of Communications, Canada, Aug 1984.

[8] W.L. Stutzman et al. "Mobile Satellite Propagation Measurements and Modeling: A Review of Results for Systems Engineers," *Proceedings of the Mobile Satellite Conference*, pp. 107-117, May 3-5 1988, Pasadena.

[9] J. Godhirsh, W.J. Vogel, "Propagation Effects by Roadside Trees Measured at UHF and L-Band for Mobile Satellite Systems, *"Proceedings of the Mobile Satellite Conference*, pp. 87-94, May 3-5 1988, Pasadena.

[10] D. C. Nicholas, "Land Mobile Satellite Propagation Results," *Proceedings of the Mobile Satellite Conference*, pp. 125-131, May 3-5 1988, Pasadena.

[11] W. Rubow, "MobileStar Field Test Program," *Proceedings of the Mobile Satellite Conference*, pp. 189-194, May 3-5 1988, Pasadena.

Appendix I

Table I shows a representative link budget for both CDMA and FDMA communicating 4800 bps to and from mobile terminals equipped with omnidirectional antennas. The assumptions on satellite position, available RF power, and antenna gain are those of [4].

The two major parameters computed through the link budget are the system capacity, i.e. the total number of simultaneous users the system can support, and the excess link margin. The calculation of the excess link margin is different for CDMA and FDMA. In the FDMA case, the excess link margin (ELM) is given by

$$ELM = E_b/N_o - \text{Fading margin} - \text{Modem loss} - \text{Mininum } E_b/N_o$$

where Minimum E_b/N_o is the theoretical signal-to-noise ratio required to support a BER=10^{-3}, Modem Loss is the implementation loss, and the fading margin is the degradation obtained in a Rician fading channel with K=10. In the CDMA case, we first calculate a Capacity Margin (CM) and then the ELM. The CM is defined as the amount by which the system capacity must be reduced in order to provide the marginal user additional $E_b/(N_o+I_o)$ and, at the same time, keep the $E_b/(N_o+I_o)$ of the nominal user a constant. To calculate the CM we have assumed the following distribution of users with the margin defined as the additional $E_b/(N_o+I_o)$ required for a BER=10^{-3} compared to an unfaded user and also ideal power control so that the faded user can utilize the additional margins.

		Margins [dB]	
		Mobile-to-Hub	Hub-to-Mobile
94%	K=10	1.6	0.7
6%	K=10, m_s=-7.5 dB, s=3 dB	8.6	6.3

The CM is then the percent of users weighted by the above margins. Straightforward calculations show that the CM for the Hub-to-Mobile link is 1.3 dB and 2.5 dB for the Mobile-to-Hub link.

Finally, the ELM is the solution to the following equation where all quantities are expressed in dB

$$10^{-Eb/(No+Io)required/10} = 10^{-(Eb/Io + CM)/10} + 10^{-(Eb/No - ELM)/10},$$

where we have assumed the ELM directly effects Eb/No but does not have any effect on Eb/Io.

Table Ia. Hub-to-Mobile Link Budget

	Hub-to-Mobile	
	CDMA	FDMA
Frequency	1549.5 MHz	1549.5 MHz
RF Power	28.1 dBW	28.1 dBW
Power Loss	-1.8 dB	-1.8 dB
Spacecraft Antenna Gain	33.8 dB	33.8 dB
EIRP	60.1 dBW	60.1 dBW
Total Capacity	**8378** Erlangs	**2850** Erlangs
Voice Duty Cycle	35%	35%
-10•log(N•Duty Cycle)	-34.7 dB	-30.0 dB
Pilot Power	-0.2 dB	N/A
EIRP/channel	25.2 dBW	30.1 dBW
Path Loss	-188.3 dB	-188.3 dB
Polarization Loss	-0.5 dB	-0.5 dB
Mobile Antenna Gain	4.0 dB	4.0 dB
Data Rate	**4,800** bits/sec	**4,800** bits/sec
-10 log(Data Rate)	-36.8 dB/Hz	-36.8 dB/Hz
Eb	-196.4 dBW/Hz	-191.5 dBW/Hz
LNA Temperature	190 °K.	190 °K.
Antenna Noise	100 °K.	100 °K.
Total Thermal Noise	290 °K.	290 °K.
Thermal Noise Density, No	-204.0 dBW/Hz	-204.0 dBW/Hz
EIRP + Mobile Gain - Losses	-124.7 dBW	N/A
% of Satellite Power in Beam	20%	N/A
10•log(% of Sat. Power)	-7.0 dB	N/A
Spreading Bandwidth	14 MHz	N/A
-10•log(Spreading BW)	-71.5 dB/Hz	N/A
Pseudo-Noise Density, Io	-203.1 dBW/Hz	N/A
Thermal, Eb/No	7.6 dB	12.5 dB
Pseudo-Noise, Eb/Io	6.7 dB	N/A
Combined, Eb/(No+Io)	4.1 dB	12.5 dB
Capacity Margin/Fading Margin	-1.3 dB	-2.0 dB
Modem Implementation Loss	-0.3 dB	-0.4 dB
Eb/(No+Io) Minimum	2.2 dB	8.0 dB
Excess Link Margin	2.0 dB	2.1 dB

Table Ib. Mobile-to-Hub Link Budget

Mobile-to-Hub

	CDMA	FDMA
Frequency	1651.0 MHz	1651.0 MHz
HPA Power	**3.0** dBW	**3.0** dBW
E/S Antenna Gain	4.0 dB	4.0 dB
Power Loss	-1.0 dB	-1.0 dB
Path Loss	-188.8 dB	-188.8 dB
Spacecraft Antenna Gain	33.8 dB	33.8 dB
Polarization Loss	-0.5 dB	-0.5 dB
Data Rate	**4,800** bits/sec	**4,800** bits/sec
-10•log(Data Rate)	-36.8 dB/Hz	-36.8 dB/Hz
Eb	-186.4 dBW/Hz	-186.4 dBW/Hz
Spreading Bandwidth	14 MHz	N/A
10•log(Data Rate/Spr. BW)	-34.6 dB	N/A
% of Users in Beam	20%	N/A
Voice Duty Cycle	35%	35%
Total Capacity	**8,378** Erlangs	N/A
Cap.•Duty Cycle•% of Users	586 Erlangs	N/A
10•log(above)	27.7 dB	N/A
Pseudo-Noise Density, Io	-193.3 dBW/Hz	N/A
Total Sat. Noise Temperature	1190.0 °K.	1190.0 °K.
Thermal Noise Density, No	-197.8 dBW/Hz	-197.8 dBW/Hz
Thermal, Eb/No	11.5 dB	16.1 dB
Pseudo Noise, Eb/Io	7.0 dB	N/A
Combined, Eb/(No+Io)	5.7 dB	16.1 dB
Fading Margin	-2.5 dB	-2.0 dB
Modem Implementation Loss	-0.3 dB	-0.4 dB
Eb/(No+Io) Minimum	**2.2** dB	**8.0** dB
Excess Link Margin	4.6 dB	5.7 dB

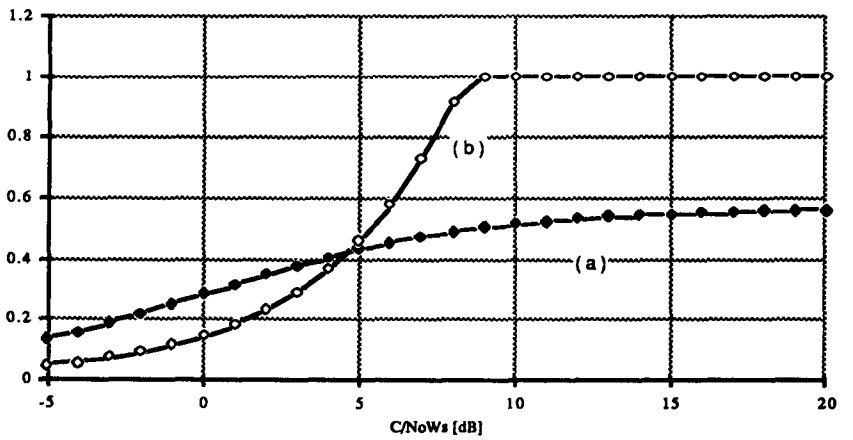

Fig. 1: Spectral efficiency in bits/sec/Hz as a function of C/N_0W_S: (a) CDMA with rate 1/3, K=9 code and E_b/N_0=2.5 dB, (b) FDMA with trellis rate 2/3, K=5, 8-DPSK and E_b/N_0=8.4 dB.

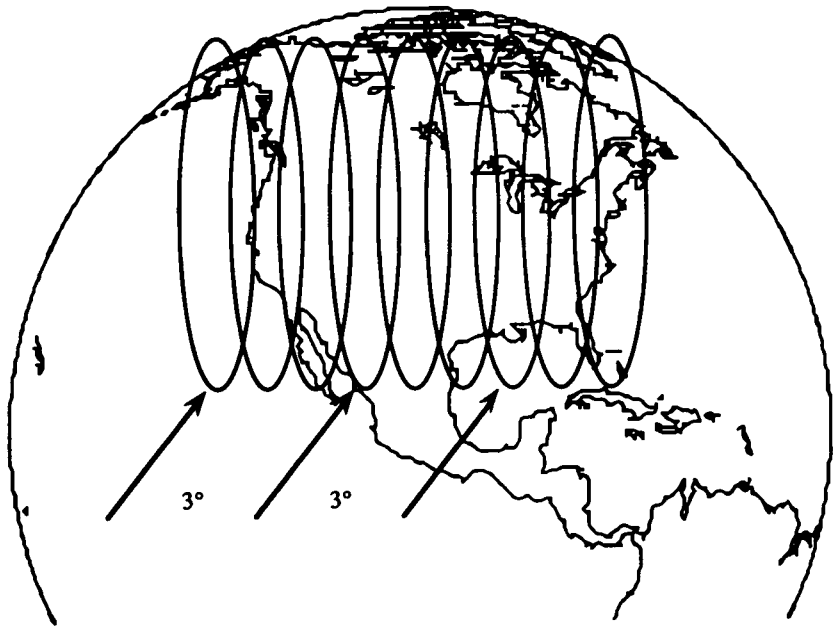

Fig. 2: Satellite antenna coverage of the continental U.S.

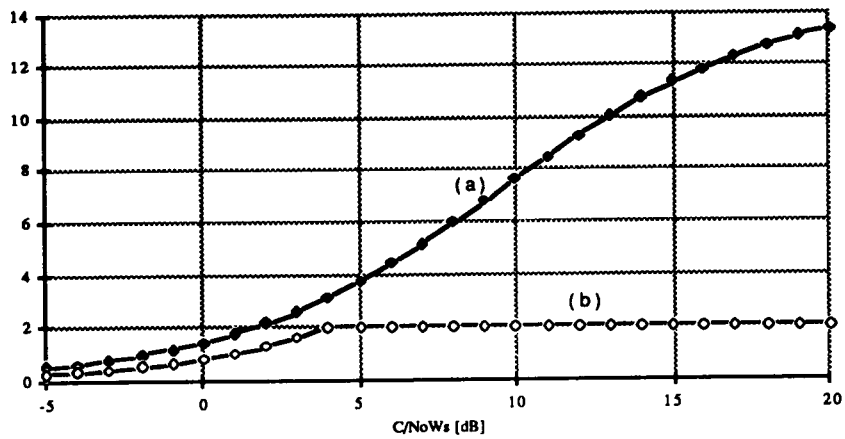

Fig. 3: Spectral efficiency in bits/sec/Hz as a function of C/N_0W_S taking into account: voice activity factor, antenna discrimination factor, and polarization reuse. (a) CDMA with rate 1/3 K=9 code and E_b/N_0=2.5 dB, (b) FDMA with trellis rate 2/3 K=5 8-DPSK and E_b/N_0=8.4 dB.

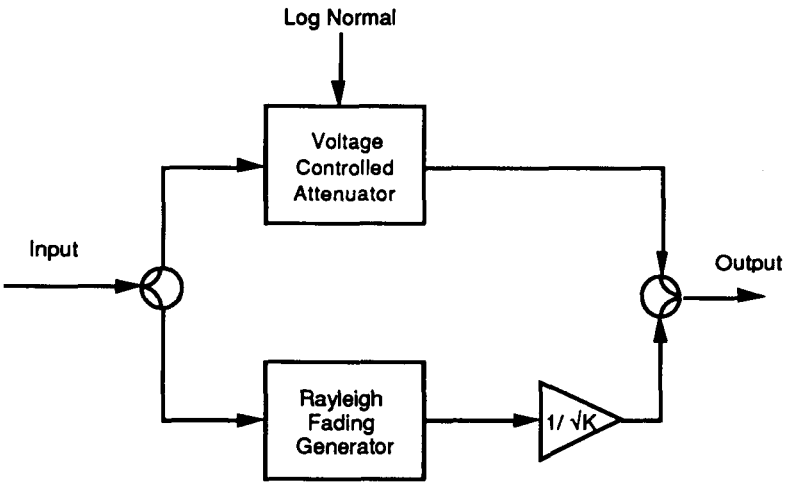

Fig. 4: Fading channel model of [7].

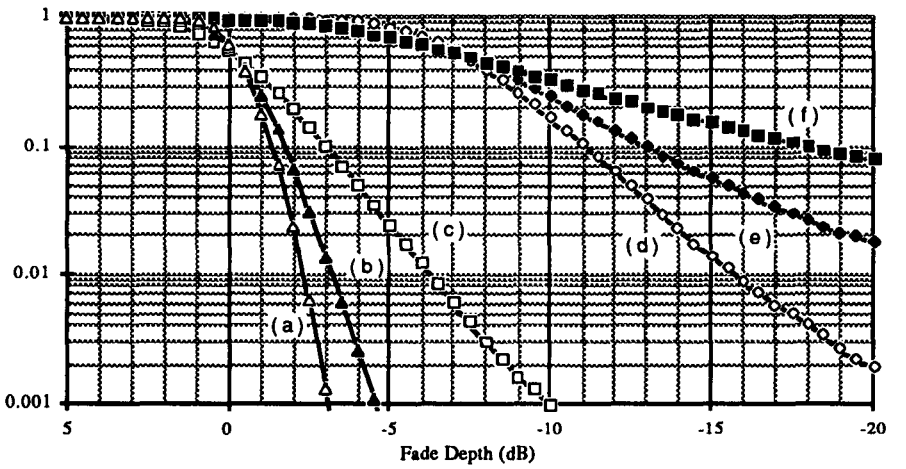

Fig. 5: Cumulative probability of fade depth simulation results obtained with the model of Fig. 4. Rician channel K=10: (a) interleaver depth=0.5 meter, (b) interleaver depth=0.26 meter, (c) without interleaver. Fading channel K=10 with shadowing m_S=-7.5 dB and s=3 dB: (d) interleaver depth=0.50 meter, (e) interleaver depth=0.26 meter, (f) without interleaver.

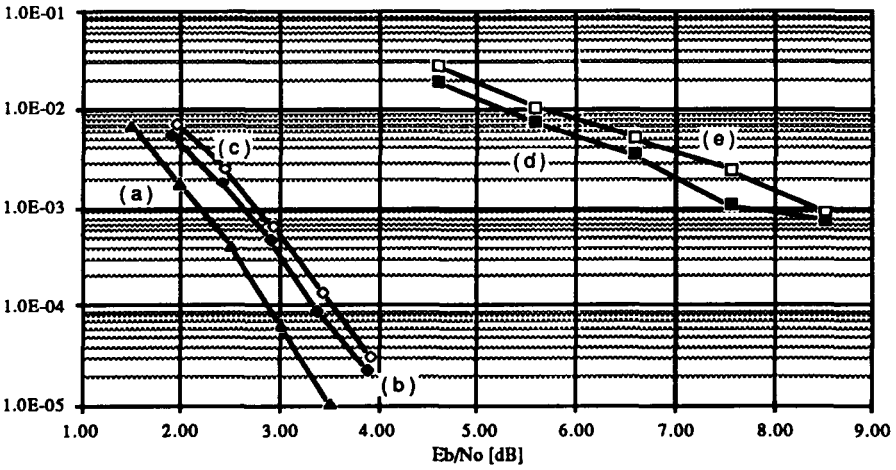

Fig. 6: Laboratory Tests Results: Hub-to-Mobile Link BER. (a) Gaussian channel theory, (b) Gaussian channel modem BER, (c) Rician fading channel with K=10 vehicle speed =48 Kmh (d) Rician fading channel K=10 with shadowing m_S=-7.5 dB σ=3 dB, vehicle speed=96 Kmh, (e) Rician fading channel K=10 with shadowing m_S=-7.5 dB σ=3 dB vehicle speed=48 Kmh. Data rate = 9600 bps, pilot $E_C/(N_O+I_O)$ = -20 dB, I_O/N_O=10 dB.

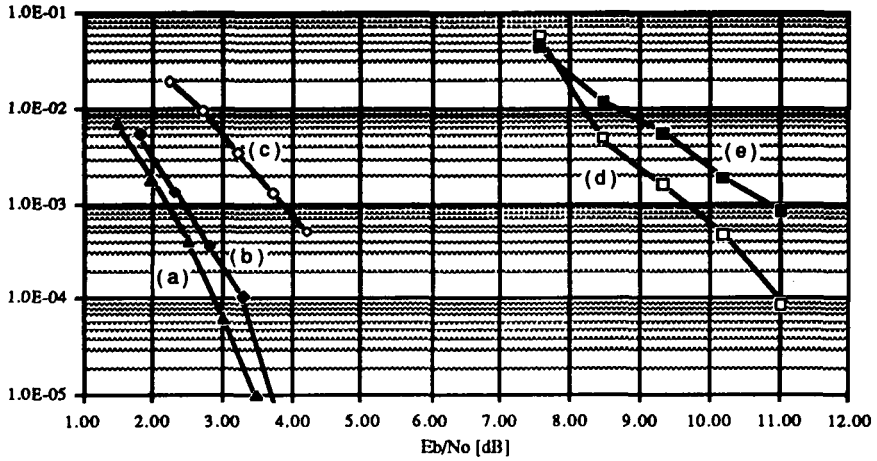

Fig. 7: Laboratory Tests Results: Mobile-to-Hub Link BER. (a) Gaussian channel theory, (b) Gaussian channel modem BER, (c) Rician fading channel K=10 vehicle speed=48 Kmh, (d) Rician fading channel K=10 with shadowing m_S=-7.5 dB s=3 dB vehicle speed=96 Kmh, DPSK, (e) Rician fading channel K=10 with shadowing m_S=-7.5 dB s=3 dB vehicle speed=48 Kmh, DPSK. Data rate = 9600 bps, I_O/N_O=10 dB.